

MODELING AND SIMULATION OF MICROSTRIP PATCH ANTENNAS VIA THE FDTD TECHNIQUE

Gonca Çakır¹

e-mail: gonca@kou.edu.tr

Levent Sevgi²

e-mail: lsevgi@dogus.edu.tr

¹ Kocaeli University, Department of Electronics & Communication Engineering, Kocaeli, Turkey

² Dogus University, Department of Electronics & Communication Engineering, Acıbadem, Istanbul, Turkey

Key words: FDTD, microstrip patch antennas, modeling, simulation

ABSTRACT

Three-dimensional finite-difference time-domain (FDTD) method is applied to full-wave analysis of microstrip patch antennas. Broadband characteristics of network parameters such as input impedance, scattering parameters are calculated from time-domain simulated data. Also radiation pattern of line-fed patch antennas are obtained. The FDTD results are first tested and calibrated against another powerful time domain simulation and then are compared with the measurements in the literature.

I. INTRODUCTION

The finite-difference time-domain (FDTD) method has been widely used in solving complex electromagnetic problems since first introduced in 1966 [1]. In FDTD, Maxwell's equations are discretized directly in space and time, and it is very flexible in modeling complex structures. Earlier applications of the FDTD were mainly in scattering, but more recently a number of researchers have applied this method to analyze broad range of electromagnetic problems from electromagnetic compatibility, to subsurface imaging, from radar cross section modeling to bio-electromagnetics [2] including antenna problems [3]. The FDTD algorithm can be used to analyze antennas of any shape, including planar and stacked microstrip antennas with probe or aperture-coupled feed effects [4].

In this study, rectangular microstrip patch array antennas are analyzed with in-house prepared FDTD package. The package is first tested and calibrated against another in-house prepared package based on the transmission line matrix (TLM) method [5]. After calibration, the package is used to investigate patch arrays. The results are compared against available measurement data.

II. PRINCIPLES OF THE FDTD

Electromagnetic fields can be described in a differential form by Maxwell equations in a linear medium,

$$\mu \frac{\partial \vec{H}}{\partial t} = -\nabla \times \vec{E} \quad (1)$$

and

$$\varepsilon \frac{\partial \vec{E}}{\partial t} = \nabla \times \vec{H} - \sigma \vec{E} \quad (2)$$

In the FDTD method, the object under investigation is directly discretized in its environment and this is called the computation volume. The smallest pieces in this volume are called cells. Each cell has a corresponding material type, which is specified in terms of the cell's permittivity, permeability and conductivity. A material may also be defined as a perfect electrical conductor (PEC), in which case the total fields in that cell are set to zero. In each cell, six electromagnetic field components E_x , E_y , E_z , H_x , H_y and H_z are located at specific points as shown in Fig. 1.

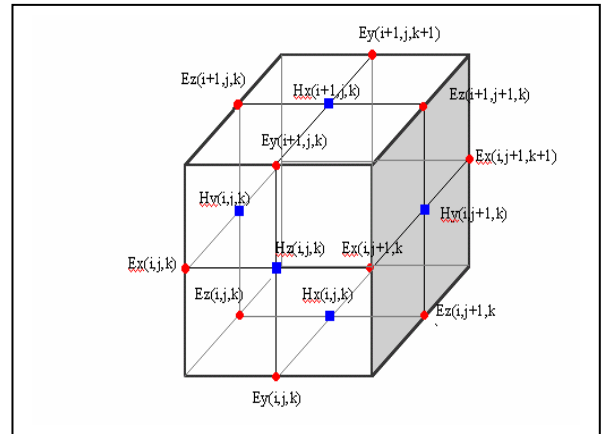


Figure 1. The 3-D FDTD unit cell

The direct output of the FDTD is information regarding the time-domain response of an antenna (or an object) to a specified source. This includes determining electromagnetic fields over space at a specific time, as well as the fields at a specific location as a function of

time. Two types of sources are of primary interest in antenna design. If a finite pulse (such as Gaussian pulse) is used, then time is advanced until the pulse fades away the computation volume. Then, a Fourier transform may be applied off-line to convert time-domain response into the frequency-domain. If, on the other hand, a single frequency sinusoid is used as the source, the simulation should be continued until the fields reach their steady state values.

Two powerful simulation packages were prepared to do tests and calibration first. They are FD-ANT and TLM-ANT, which are based on the FDTD and TLM methods, respectively. Sample microstrip structures are used for these tests and scattering parameters are calculated via both packages. Typical results are pictured in Figs 2 and 3, together with the structures under investigation.

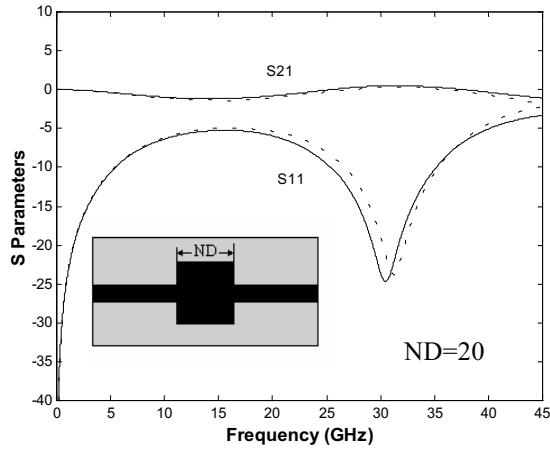


Figure 2. S parameters vs. frequency simulated via FD-ANT and TLM-ANT packages - 1

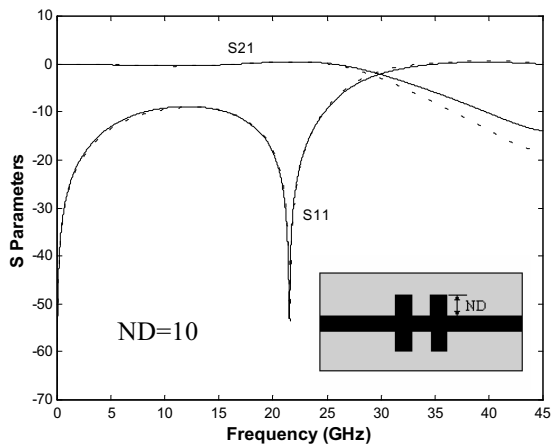


Figure 3. S parameters vs. frequency simulated via FD-ANT and TLM-ANT packages - 2

Here, $60 \times 24 \times 100$ FDTD space is used with $\Delta x = \Delta y = \Delta z = h/6$, where $h = W = 1$ mm (h : height of the substrate, W : width of the microstrip line). Time step

$\Delta t = \Delta x / (2c)$, where c is the speed of light in vacuum. Relative permittivity is fixed to 2.2. As observed in these examples, a very good agreement has been obtained between results of the packages.

III. FDTD ANALYZES OF PATCH ANTENNAS AND NUMERICAL IMPLEMENTATION

After calibrating the FD-ANT package against the TLM-ANT, numerical simulations have been performed for two configurations; a line-fed rectangular patch antenna and three-element patch coplanar parasitic microstrip antenna [6,7]. Schematic diagrams of microstrip patch antennas analyzed with the FD-ANT package are shown in Fig. 4.

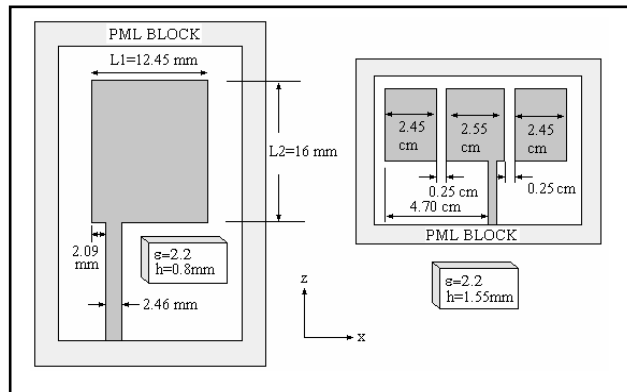


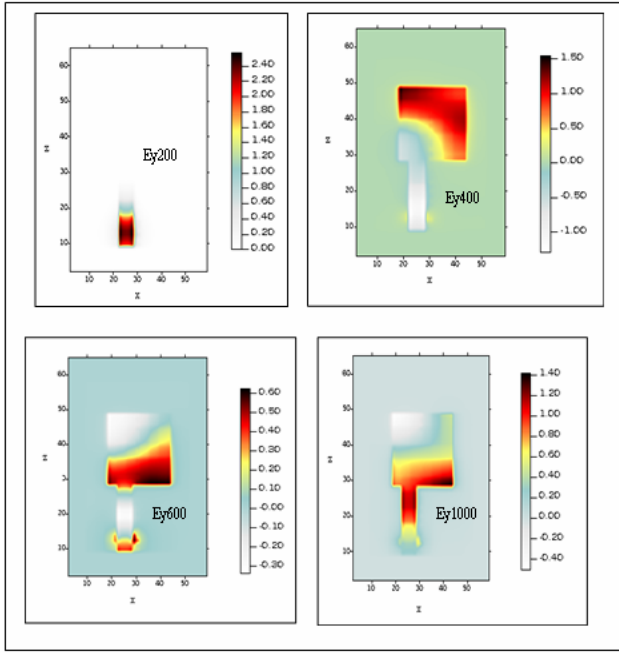
Figure 4. Structures of Line-fed rectangular and three-element coplanar patch parasitic microstrip antennas

The line-fed rectangular patch is designed to have a resonant frequency at 7.5 GHz, and the second one is at 3.9 GHz. These patches are etched on a dielectric substrate with $\epsilon_r = 2.2$. The length of the fed-line from the source plane to the edge of the antenna is $20\Delta z$, and the reference plane for port 1 is $10\Delta z$ from the edge of the patch for both of antennas. Berenger's perfectly matched layer (PML) with 8 cells is applied as the absorbing boundary condition. Other parameters of the structures are given in Table 1.

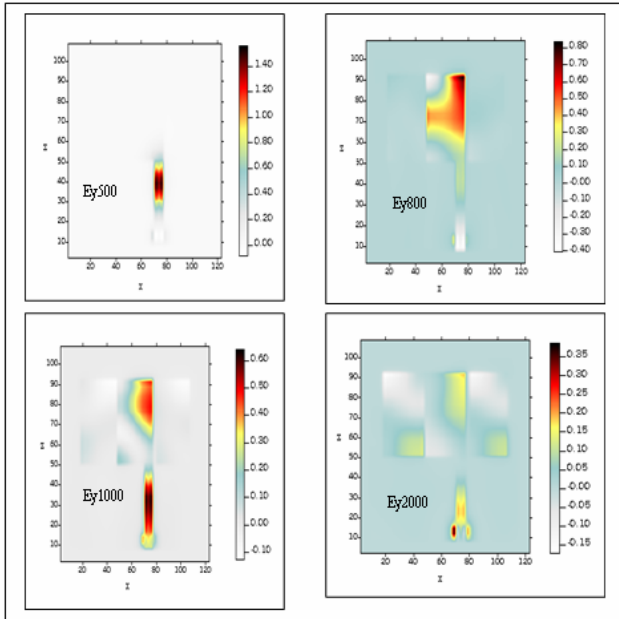
Table 1. The parameters of patch antennas

	Line-fed single patch	Array antenna
Substrate thickness	0.8 mm	1.55 mm
Space Steps	$\Delta x = 0.492$ mm	$\Delta x = 0.15$ cm
	$\Delta y = 0.198$ mm	$\Delta y = 0.038$ cm
	$\Delta z = 0.8$ mm	$\Delta z = 0.15$ cm
Total Size	NX=60	NX=89
	NY=20	NY=20
	NZ=66	NZ=76

The spatial distribution of $E_y(x,y,z,t)$ just beneath the microstrip antennas at difference time steps are shown in Fig. 5.



(a)



(b)

Figure 5. Time variation of E_y at the z - x plane in the substrate, (a) for a line-fed rectangular patch, (b) for a three-element coplanar patch antenna

Microstrip patch antenna is a one-port circuit. Its scattering matrix has only one element, that is, S_{11} or the reflection coefficient. S_{11} is defined as

$$S_{11}(f) = \frac{V_{ref}(f)}{V_{inc}(f)} \quad (3)$$

where $V_{ref}(f)$ is the Fourier transformed reflection voltage at the input plane, and $V_{inc}(f)$ is the Fourier transformed incident voltage at the same position [7]. The scattering coefficient results of the rectangular patch antenna, shown in Fig. 6.

The operating resonance at 7.5 GHz is strongly traced via both the FD-ANT simulation package and in the measurement. The results are in good agreement.

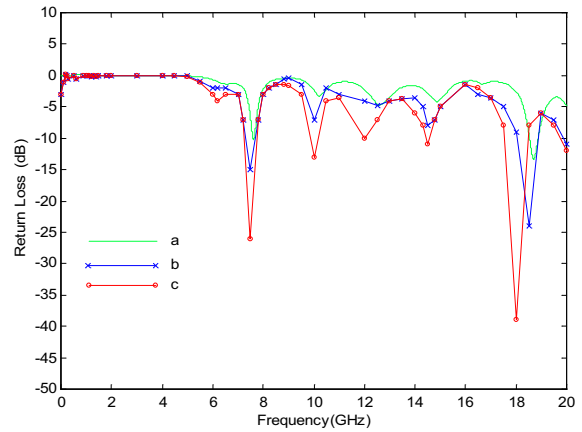


Figure 6. Return loss vs. frequency of the line-fed rectangular antenna, (a) FD-ANT result, (b) measurement result from [6], (c) FDTD result from [6]

Return loss vs. frequency of the three-element microstrip patch antenna is shown in Fig. 7. As shown in the figure, resonance frequency of the patch array is at about 3.9 GHz. Our FDTD result is in good agreement with measurement.

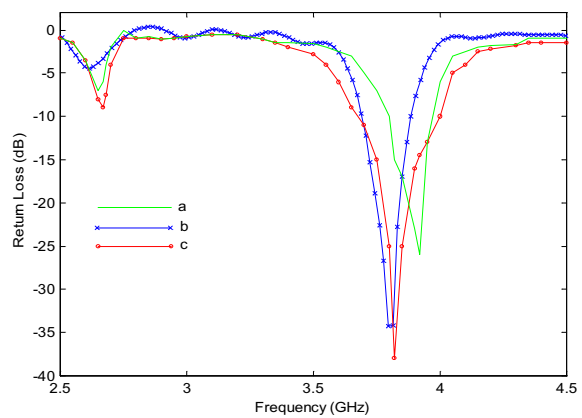


Figure 7. Return loss vs. frequency of the three-element patch array (curve legends same with Fig. 6)

Input impedance of an antenna may be calculated from the computed $S_{11}(f)$ by transforming the reference plane to the edge of the microstrip antenna as,

$$Z_{in} = Z_0 \frac{1 + S_{11} \cdot e^{j2kL}}{1 - S_{11} \cdot e^{j2kL}} \quad (4)$$

where k is the wavenumber on the microstrip, L is the length from the edge of the antenna to the reference plane ($10 \Delta z$), and Z_0 is the characteristic impedance of the microstrip line [4]. Input impedances of the antennas calculated in this manner are shown in Fig. 8.

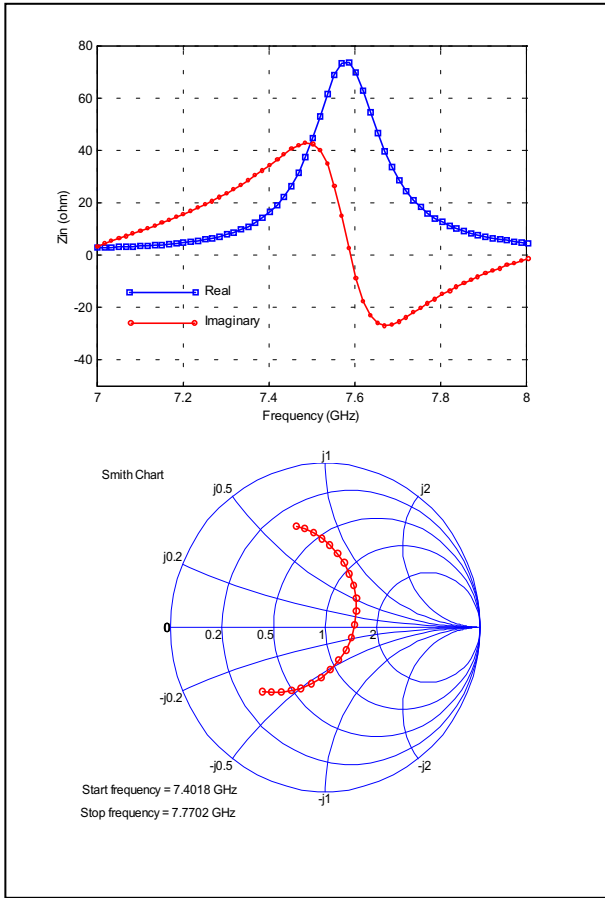


Figure 8a. Input impedance vs. frequency of the patch antenna

Relatively narrow and broad band characteristics around the resonance frequencies are clearly observed in Figs. 8a and 8b, respectively.

Finally, radiation patterns of both the patch and three-element patch array antenna are simulated via FD-ANT and are plotted in Fig. 9a and 9b, respectively. Here both patterns belong to yz -plane radiation for the theta components of the electric field. Nearly 60 degrees beam width is obtained with a single patch for the parameters listed in Table 1. On the other hand, locating two nearby parasitic patches as given in Fig. 4 results in a narrower

beamwidth as illustrated in Fig. 9b. The more parasitic (or line-fed) elements in the array the narrower the beamwidth.

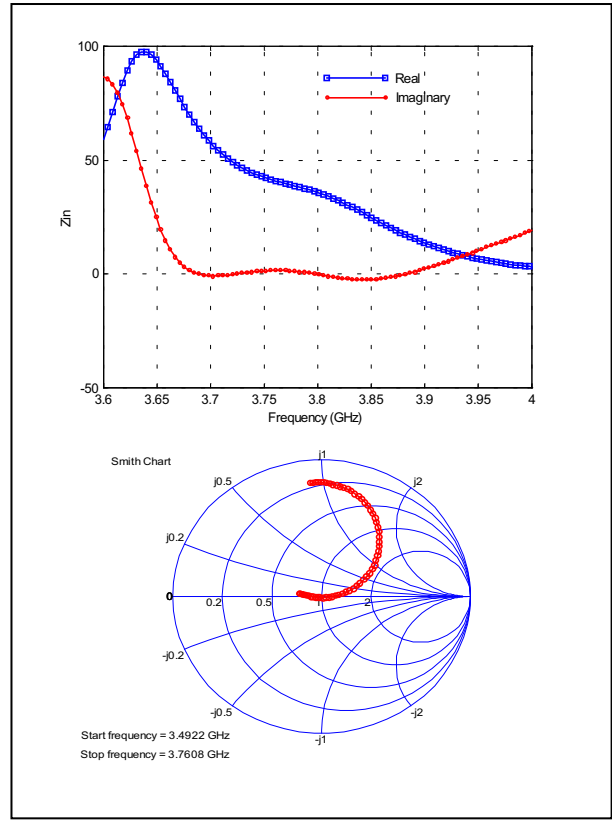


Figure 8b. Input impedance vs. frequency of the patch array

It should be noted that an effective near-to-far field transformation package is accommodated into the FD-ANT package to deal with the radiation patterns. Moreover, the patch is discretized and located in free-space in the computation volume which is terminated by effective PML-type absorbing boundary simulators.

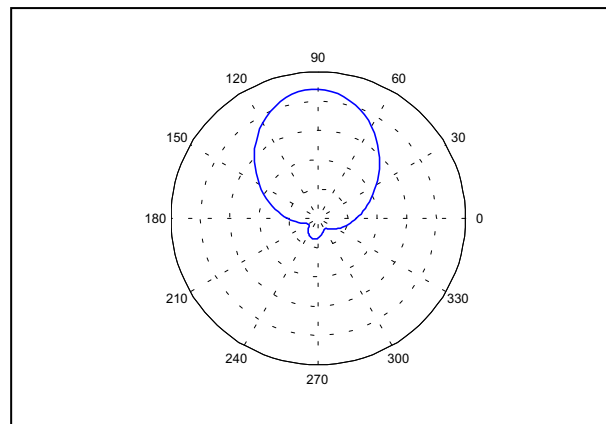


Figure 9a. Radiation patterns (on yz -plane) of the microstrip patch antenna

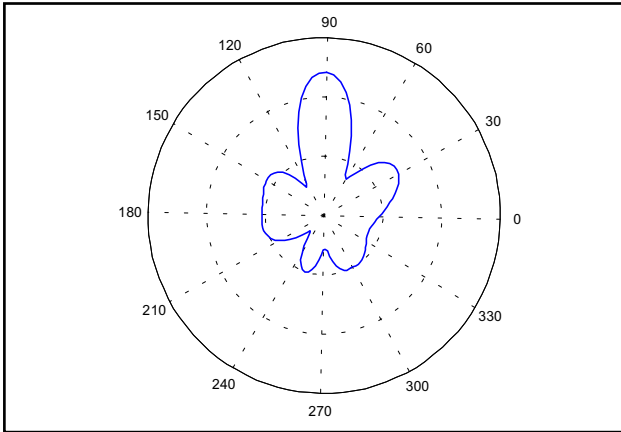


Figure 9b. Radiation patterns (on yz-plane) of the three-element microstrip patch array

IV. CONCLUSIONS AND DISCUSSION

Canonical microstrip patch structures are investigated in this study with an in-house prepared FDTD antenna package, FD-ANT. The package is first tested and calibrated against another package prepared in our group, the TLM-based antenna simulation package. After the calibration example structures are investigated in detail.

The FD-ANT package deals with network parameter computations which requires near field simulations, as well as radiation pattern simulations which require near-to-far field transformation routines. In FD-ANT, near-to-far field transformation is directly performed in time-domain while the FDTD simulation runs. Off-line discrete Fourier transformation is applied to the FDTD data in order to obtain frequency-domain characteristics when the simulation is over. It is shown here that the FDTD method is very effective in simulating microstrip patch antenna arrays.

REFERENCES

1. K. S. Yee, "", IEEE Trans. Ant. Propagat., Vol. AP-14, No. 3, pp.302-307, May 1966
2. Levent Sevgi, "Complex Electromagnetic Problems and Numerical Simulation Approaches", IEEE Press, Piscataway, New Jersey, USA, 2003
3. A. Reineix and B. Jecko, "Analysis of Microstrip Patch Antennas Using Finite-Difference Time Domain Method", IEEE Trans. Ant. Propagat., Vol. AP-37, pp.1361-1369, Nov. 1989.
4. Martin L. Zimmerman, "Use of the FDTD Method in the Design of Microstrip Antenna Arrays", Int.J. of Microwave and Millimeter-wave Comp.-aided eng., Vol.4, No.1, 58-66, 1994.
5. M. Orhan Özyalçın, "Modeling and Simulation of Electromagnetic Problems via Transmission Line Matrix Method", Ph.D. Dissertation, Istanbul Technical University, Institute of Science, October 2002
6. David M. Sheen, S.M. Ali, M. D. Abouzahra, J. A. Kong, "Application of Three-Dimensional Finite-Difference Time-Domain Method to the Analysis of Planar Microstrip Circuits" IEEE Trans. On Microwave Theo. And Tech., vol.38, No.7, July 1990.
7. X. Zhang, K. K. Mei, "Time-Domain Finite Difference Approach to the Calculation of the Frequency-Dependent Characteristics of Microstrip Discontinuities", IEEE Trans. On Microwave Theo. And Tech., vol.36, No.12, December 1988.